

Energy deposition and heat diffusion in the process of chalcogenide glass modification by femtosecond laser pulses

Elena Romanova (1), Andrey Konyukhov (1), Sergey Muraviov (2), Grigory Gelikonov (2)

1) Saratov State University, Russia, romanova@optics.sgu.ru

2) Institute of Applied Physics of RAS, Nizhny Novgorod, Russia

Abstract: *The process of energy deposition in highly non-linear chalcogenide glasses by focused femtosecond pulses, heat diffusion and subsequent cooling of the illuminated volume are investigated in a theoretical model as well as in experiments.*

Introduction

Direct photo-fabrication of optical waveguides by femtosecond (fs) laser pulses in bulk materials enables the dawn of a new generation of optical devices, which are potentially cheap and allow for a dense integration due to the 3D character.

When a femtosecond pulse is tightly focused in a transparent material, the energy is deposited in a small volume around the focus due to multiphoton absorption. The photo-generated hot electron plasma rapidly transfers its energy to the lattice, giving rise to high temperatures and pressures. This produces, by a mechanism still under investigation, a local material densification with an increase or decrease of refractive index, depending on the glass composition. The unclear mechanism of refractive index variation is currently the main drawback in the theoretical treatment of the modifications of the optical properties of glasses via exposure to fs pulses. In [0] the glass modification was associated with the heating process. A thermal diffusion model accurately tracks the waveguide diameter. However theoretical model in [1] does not take into account pulse propagation dynamics and pulse nonlinear absorption. For proper description of the shape of the modified glass region the glass phase transition during the thermal diffusion should be considered also.

In this paper, we study the process of energy deposition into highly non-linear (chalcogenide) glass by focused fs pulse and subsequent heat diffusion outside the illuminated volume. The theoretical treatment is based on the model of fs pulse propagation in non-linear dielectric medium [2]. Spatiotemporal dynamics of the pulse is described by the 2D+T parabolic wave equation where we used the Pade approximation with respect to longitudinal coordinate to take into account wide-angle radiation of the tightly focused laser beam. In the model, we assume that permanent change of the refractive index is associated with heating of the glass sample up to the glass transition temperature T_g , subsequent cooling and solidification. After illumination, variation of the absolute temperature T with time is described by the heat diffusion equation with account of heat flow on

the moving boundary between solid and liquid phases in a glass sample.

We are presenting also the experimental results of chalcogenide glass modification by fs pulses of 1.55 μm fibre laser (pulse duration 150 fs, repetition rate 25 MHz). The AsSe glass chemical composition has been tailored by doping with germanium or tellurium. For characterisation of the refractive index variation upon the glass modification, the optical coherent tomography has been used.

Non-linear absorption of focused fs pulses

Spatiotemporal dynamics of the pulse is described by the 2D+T parabolic wave equation for the slowly varying envelope $E(z, r, \tau)$ of electrical field:

$$\frac{\partial}{\partial z} \left(1 + \frac{1}{2ik} \frac{\partial}{\partial z} \right) E + \frac{1}{2ik} \left(\nabla_{\perp}^2 E - \frac{2}{u} \frac{\partial^2 E}{\partial z \partial \tau} \right) = \left(iP_{\text{nl}} - \frac{2}{\omega_0} \frac{\partial P_{\text{nl}}}{\partial \tau} \right) - i \frac{\beta_2}{2} \frac{\partial^2 E(z, r, \tau)}{\partial \tau^2} - j_{\text{nl}}, \quad (1)$$

where we use the Pade approximation with respect to longitudinal coordinate. The second order derivative $\partial^2 E / \partial z^2$ was included into the left-hand-side of Eq.(1) to prevent beam collapse due to Kerr self-focusing. In Eq. (1), $k = \omega_0 / u$ is the mean wavenumber (u is the light velocity in glass, $\tau = t - z/u$ is the time in the moving coordinate system, ω_0 is the pulse carrier frequency), β_2 is the group-velocity dispersion. In the expression for the nonlinear polarization P_{nl} , we include the effects of the nonlinear refractive index change and energy deposition through formation of electron plasma density ρ :

$$P_{\text{nl}}(z, r, \tau) = \gamma |E|^2 E + i \frac{\alpha_p}{2} (\delta_1 \rho + |E|^2 \rho^{(p-1)}) E, \quad (2)$$

$\gamma = n_2 \omega_0 / c$, $n_2 = 1.8 \times 10^{-14} \text{ cm}^2/\text{W}$ is the Kerr constant, α_p is the p -photon absorption coefficient. For chalcogenide glasses which have bandgap edge at 1.24 eV the major role in nonlinear absorption of $\lambda = 1.55 \mu\text{m}$ radiation plays the two-photon absorption ($p=2$, $\alpha_p = 0.6 \text{ cm/GW}$).

The current density is defined by equation

$$\frac{\partial \rho(z, r, \tau)}{\partial \tau} = \delta_1 \rho |E|^2 + |E|^2 \rho^p - \delta_2 \rho^2, \quad (3)$$

where the first term on the right-hand-side describes growth of the electron plasma by cascade (avalanche) ionization, the second term is the contribution of multiphoton absorption, which acts both as a source for the cascade process and as a contributor to plasma

growth, and the third term describes the radiative electron recombination. Evolution of plasma in glass is described by the Drude model [3]:

$$j_{nl}(z, r, \tau) = i \frac{1}{L_{pl}} \left(1 - \frac{i}{\omega_0 \tau_c} \right) \left(E - \frac{\tau_c}{1 - i\omega_0 \tau_c} \frac{\partial E}{\partial \tau} \right) \rho, \quad (4)$$

where τ_c is the electron-collision time ($\omega_0 \tau_c = 5$), $L_{pl} = 1 \mu\text{m}^{-1}$ is the plasma length. In Eq. (4), plasma diffusion is not taken into account because we consider here fs pulses with so short time scales that plasma diffusion (characteristic time $\sim 1 \mu\text{s}$) occurs after the pulse has left the region of focusing.

Heat diffusion in glass

Energy deposition into the glass sample by a fs pulse results in temperature increase inside the illuminated volume. To study the dynamics of glass heating upon a fs pulse irradiation, a model of thermal diffusion was used. After irradiation, spatial variation of the absolute temperature T with time t is described by the equation:

$$\left(c(T) + \Lambda \delta(T - T_g) \right) \frac{\partial T}{\partial t} = \frac{1}{r} \frac{\partial}{\partial r} \left(K(T) r \frac{\partial T}{\partial r} \right), \quad (5)$$

where $c = \rho_g C$ is temperature-dependent coefficient, C is specific heat capacity, ρ_g is the glass density, Λ is enthalpy, $\delta(T - T_g)$ is the unit impulse function, K is temperature-dependent heat conductivity. The temperature dependency of the coefficients take into account glass phase change at $T = T_g$.

$$c(T) = \begin{cases} c_1, & T < T_g \\ c_2, & T > T_g \end{cases}, \quad K(T) = \begin{cases} K_1, & T < T_g \\ K_2, & T > T_g \end{cases}, \quad (6)$$

where $c_1 = 1.47 \text{ J}\cdot\text{cm}^{-3}\cdot\text{K}^{-1}$, $c_2 = 1.76 \text{ J}\cdot\text{cm}^{-3}\cdot\text{K}^{-1}$, $K_1 = 0.3 \times 10^{-2} \text{ W}\cdot\text{cm}^{-1}\cdot\text{K}^{-1}$, $K_2 = 0.25 \times 10^{-2} \text{ W}\cdot\text{cm}^{-1}\cdot\text{K}^{-1}$, $\Lambda = 23.6 c_1$. Stepwise function for $c(T)$ and $K(T)$ was used, because detailed information concerning thermal properties of chalcogenide glasses was not available. The initial temperature variation is defined as

$$\Delta T = W / c, \quad (7)$$

where W is energy density of the heat source. The heat source due to a fs pulse irradiation can be considered as a delta function in time because the pulse duration is much less than the characteristic time of the heat diffusion ($\sim 1 \mu\text{s}$).

In our model, we assume that permanent change of refractive index is associated with heating of the glass sample up to the glass transition temperature T_g due to the energy deposition by a fs pulse, subsequent cooling and solidification of the illuminated region.

Numerical results

In numerical simulations, non-stationary Gaussian beam ($\lambda = 1.55 \mu\text{m}$) was focused at the depth $200 \mu\text{m}$ from the surface of bulk glass sample (focal spot dimension of low-intensity beam $\sim 1 \mu\text{m}$). Initial temporal distribution was taken *sech*-shaped with the half-width (pulse duration) 100 fs .

The energy deposition and spatial distribution of heat sources inside the irradiated volume depend mostly on a balance of self-focusing, multi-photon absorption and plasma defocusing. It doesn't depend significantly on splitting of the pulse at the focus resulting from the self-steepening and space-time focusing effects because energy of the heat sources is calculated by integration of pulse temporal envelope at each point of the illuminated volume.

Numerical results

Strong multiphoton absorption of the pulse energy arises before the focal plane (Fig.1, $180 < z < 200 \mu\text{m}$). Full absorbed energy increases with initial pulse energy that fits the available experimental results [4]. The pulse energy absorption increased sufficiently when the beam becomes strongly self-focused (Fig.2).

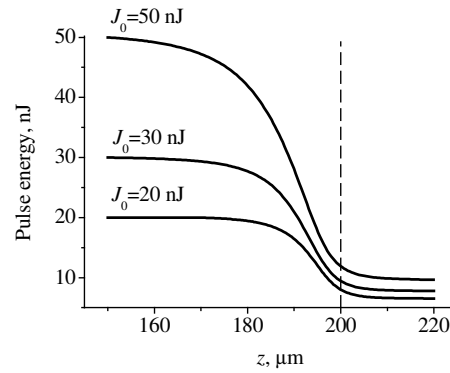


Fig.1: Pulse energy absorption. J_0 is the energy of input pulse. Vertical dashed line shows the focal plane inside the glass.

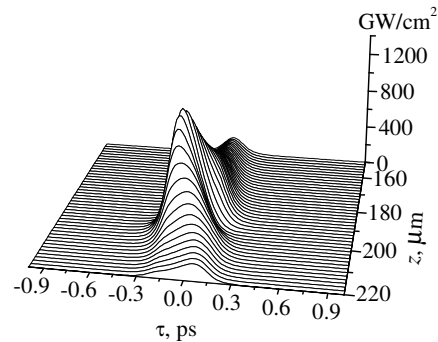


Fig.2: Intensity on the beam axis. Energy of input pulse is 50 nJ .

The multiphoton absorption, self-steepening and plasma formation lead to distortion of the pulse shape. In spite of the high intensity on the beam axis the propagation distance is not sufficiently large to obtain significant pulse spectral broadening due to self-phase modulation (Fig.3). After the focal plane ($z > 200 \mu\text{m}$) the beam become strongly divergent and

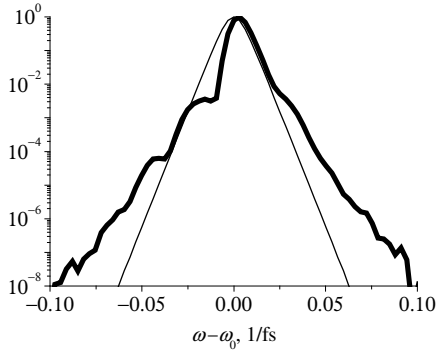


Fig.3: Spectral intensity on the beam axis. Initial pulse spectrum (thin curve) and pulse spectrum after propagation distance 220 μm (thick curve). Energy of input pulse is 50 nJ.

local intensity rapidly decreases. As result the effect of the nonlinear processes become inappreciable. For considered pulse energies the pulse shape and pulse spectrum practically does not change after focal plane.

In Fig.4, contour lines correspond to $T_g = 180^\circ\text{C}$ (chalcogenide glass) measured at some moments of time t after irradiation. At $t=0$, shape and dimensions of the initially melted region ($T > T_g$) can be tailored by enhancing or decreasing the self-focusing with respect to the plasma defocusing. The increase of the energy of input pulse shifts the region $T > T_g$ backward to the pulse source, because with the higher energy pulses the multiphoton absorption starts at the shorter propagation distances (Fig.1). For the pulse energy equal to 50 nJ the temperature is at a maximum at the point $r=0$, $z=196 \mu\text{m}$, while for pulse energy 20 nJ this point is $r=0$, $z=197 \mu\text{m}$.

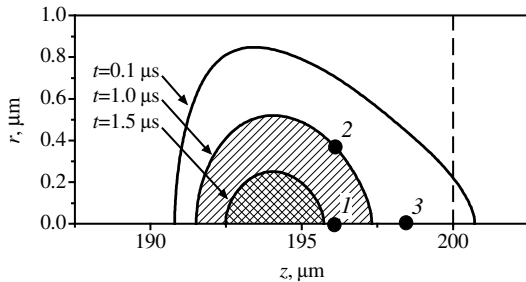


Fig.4: Contour lines $T=T_g$ at the different time after radiation by single 100 fs pulse. Initial pulse energy is 50 nJ. Vertical dashed line shows focal plane of the focusing lens. The temperature dynamics at three black points shown in the Fig.5.

Both the region restricted by the curve $T=T_g$ ($t \leq 0.1 \mu\text{s}$, Fig.4) and experimentally observed laser-induced refractive index change [1] have drop-like shape.

While glass is cooling, the T_g lines move inside the irradiated region (Fig.4). Structural changes upon transformation of hot viscous liquid into solid glass

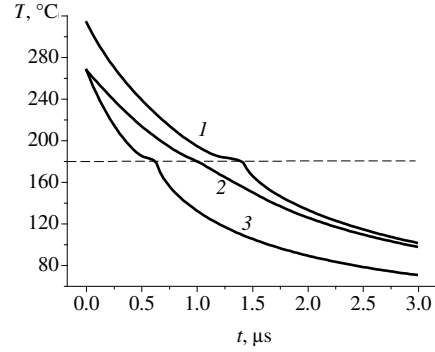


Fig.5: Temperature dynamics at the three different spatial points (see Fig.4). Dashed line shows $T=T_g$.

depend on the cooling rate. We show that the cooling rate is greater at the beam axis than at the periphery (Fig.5) that is associated with the ellipsoidal shape of the modified region (Fig.4). Due to the glass phase transition (6) the cooling rate at $T=T_g$ is slowed down (on-axis points 1 and 3, Fig.5). The cooling rate can be also tailored by variation of the pulse energy and pulse repetition rate so that the motion of T_g lines can be managed to provide better cooling conditions.

Up to $t=1.3 \mu\text{s}$ the length and radius of modified region decrease linearly (Fig.6). For $t > 1.3 \mu\text{s}$ r_m and z_m decrease rapidly to zero.

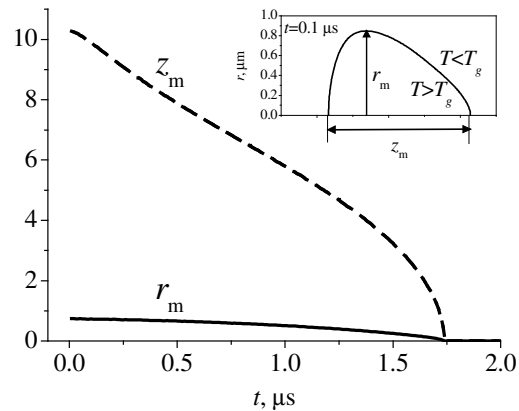


Fig.6: Radius r_m (solid curve) and length z_m (dashed curve) of modified region versus time. Inset show the method of determining r_m and z_m .

Experiments

In experiments (Fig.7), glass samples were locally illuminated by 150 fs laser pulses with mean wavelength at 1.55 μm .

Three kinds of glasses were used: $E_g=1.72 \text{ eV}$, $T_g=185^\circ\text{C}$ ($\text{As}_{40}\text{Se}_{60}$, oxygen gettered glass), $E_g=1.51 \text{ eV}$, $T_g=205^\circ\text{C}$ ($\text{Ge}_{17}\text{As}_{18}\text{Se}_{65}$ glass) and $E_g=1.27 \text{ eV}$, $T_g=265^\circ\text{C}$ ($\text{Ge}_{17}\text{As}_{18}\text{Se}_{56}\text{Te}_9$ glass), where E_g is the band edge. Mean power of the Er^{3+} doped fibre laser was varied in the range 2.0–8.0 W.

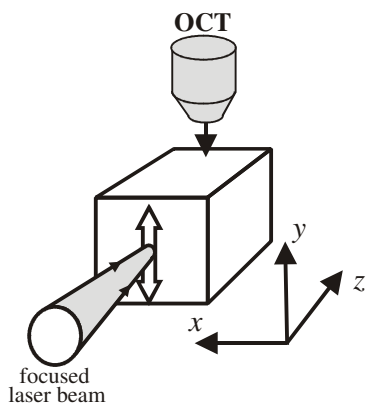


Fig.7: Experimental setup. The glass was modified inside the sample by focused laser pulses. The $\lambda=1.55\ \mu\text{m}$ radiation was focused by $60\times$ microscope objective. During the glass modification process the glass sample was translated in y -direction. The change of refractive index was detected by optical coherent tomography (OCT).

Results of the illumination were characterised by the optical coherent tomography.

Behaviour of the illuminated regions inside glass demonstrated strong dependence on the glass composition. We have found thresholds for irreversible glass modifications which decrease significantly with linear bandgaps. For some range of powers below the bandgaps, reversible modifications have been found by observation of diffraction patterns on a screen. These diffraction patterns disappeared within few seconds. However for a range of powers above the bandgaps, the diffraction patterns were stable. Changes of the refractive index over the modified regions were observed (Fig.8) by optical coherent tomograph (3D spatial resolution $10\ \mu\text{m}$ at wavelength $1.3\ \mu\text{m}$, scanning time 1 s, scanning depth 2-3 mm, sensitivity for refractive index changes 0.001).

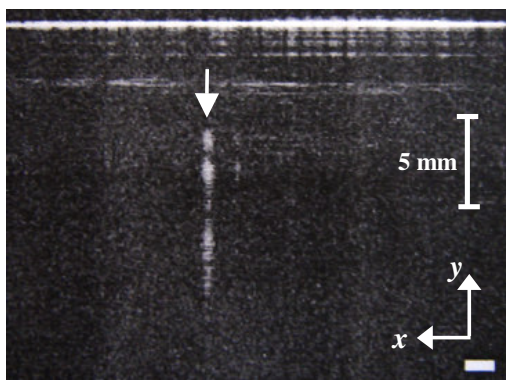


Fig.8: OCT image of a refractive index change. Laser direction is normal to page. Pointer shows the modified area.

Variations of the refractive index in the spots are due to variation of the focusing conditions during the sample illumination.

The threshold powers for irreversible modifications were found significantly lower for lower bandgap glasses (0.1–1 W). Increase of the power above the damage threshold resulted in ablation and glass evaporation. For $\text{Ge}_{17}\text{As}_{18}\text{Se}_{65}$ glass, the range of powers between the threshold for modification and ablation was extremely small (6-7 W).

Conclusions

In the paper, we have presented theoretical model for glass modification by fs laser pulses and applied this model to study energy deposition and heat diffusion in chalcogenide glasses. In parallel, we have studied the thresholds for chalcogenide glass modifications in experiments using Er^{3+} fibre laser and optical coherent tomograph.

The results demonstrated great flexibility of the technology that can be achieved by tailoring glass composition and illumination conditions. Temporal dependences of the glass cooling over the illuminated region provide insight into the photo-structural process and can be used together with Differential Thermal Analysis for better understanding of modification process in different glasses. The results obtained by optical coherent tomograph prove efficiency of this technique in characterisation of the complicated 3D structures for photonics.

Acknowledgments

The authors gratefully acknowledge Professor A. Seddon, Professor T. Benson and Dr. D. Furniss from the University of Nottingham for the glass samples which they kindly provided for the experiments, for helpful discussions and collaboration in this research field.

References

- 1 S. Eaton et al, *Opt. Express*, v. 13, no. 12, p. 4708, 2005
- 2 K. Moll, A. Gaeta, *Opt. Lett.*, v. 29, p. 995, 2004
- 3 Q. Feng et al, *IEEE J. of Quant. Electron.*, v. 33, no. 2, p.127, 1997
- 4 A. Alexandrov et al., *Quant. Electron.*, v. 31, p. 398, 2001.